Chapter

Green Comparable Alternatives of Hydrazines-Based Monopropellant and Bipropellant Rocket Systems

Dov Hasan, Dan Grinstein, Alexander Kuznetsov, Benveniste Natan, Zohar Schlagman, Avihay Habibi and Moti Elyashiv

Abstract

Concepts are presented for "green" (with reduced hazards) replacements for monopropellant hydrazine propulsion systems and for hypergolic bipropellant systems while maintaining similar performance. At the onset of the "green propulsion" age, "green" alternatives to hydrazine propulsion have been emerging. The introduction rate of these into space systems is very slow due to the conservatism of the space propulsion industry. The concept presented here for monopropellant hydrazine systems offers gradual conversion to "green propellants" by dual capability of conventional hydrazine systems and ammonium dinitramide (ADN)-based systems. An initial risk reduction program has been carried out for materializing the concept. It includes proof of concept of dual use of all propulsion system parts. Materials compatibility and actual operation have been demonstrated. For bipropellants, we present the emerging "green" hypergolic system based on kerosene and peroxide, similar in performance to MMH/N_2O_4. Results of the proof-of-concept and development model systems are presented. The experimental results of various engine types demonstrate the capability to operate in both pulse and steady-state modes and the ability to produce different thrust levels. The fuel and oxidizer show very robust hypergolicity and short ignition delay times, as well as characteristic velocity efficiency exceeding 98%.

Keywords: green propulsion, hypergolic, space propulsion, rocket, thruster, H_2O_2, kerosene, hydrazines

1. Introduction

The use of chemical propulsion systems for rocket engines is quite common for over half a century. Hydrazines are the major chemical space propellants of choice due to their good performance and reliable track record. A majority of low earth orbit (LEO) satellite propulsion systems are based on monopropellant hydrazine thrusters. The Israeli Offek LEO satellites employ such a hydrazine system [1–3]. **Figure 1** depicts the Offek satellite top plate with monopropellant hydrazine thrusters, being the space facing part of the propulsion module. **Figure 2** depicts the propulsion system module and its schematic, which identify the construction and major parts and components of a typical monopropellant space propulsion system.

Hazards have been identified as an elemental part of such work with materials, which for the sake of performance are required to react as energetically as possible. The hazards are part of the technology throughout the life cycle, from manufacturing, handling, transport, and storage, through actual firing in rocket motors and eventually disposal.

The term "green propellants" has been generally used to describe propellants that have the benefit of reducing any of the abovementioned hazards. Based on the European Space Agency (ESA) definition, a "green propellant" is one that has the potential to have reduced adverse impact, either to the environment or to personnel with whom it may come into contact, while still having the performance to meet mission requirements. The term "reduced hazard propellant (RHP)" has been appropriately coined to describe the propellants for which any of the hazards are reduced.

As part of the ongoing deepening and widening of safety concerns throughout the world, there is an ongoing regulatory process in Europe, which has brought about the subject of RHP to be of high priority. This includes decisions at the European Parliament level of the establishment of the European Chemical Agency (ECHA) and to effect the regulation REACH for Registration, Evaluation, Authorization and Restriction of Chemicals in Europe in mid-2007 [4, 5].

At the onset of the "green propulsion" age, RHP alternatives to propulsion have been emerging. The introduction rate of these into space systems is very slow due to the conservatism of the space propulsion industry [6]. The only "green" satellite propulsion technology that has to date gained actual space heritage as monopropellant replacement is the ADN-based monopropellant by ECAPS that made its debut in 2010 aboard the Swedish Prisma satellite and was recently launched aboard the American SkySat constellation [7–18]. While the ADN-based monopropellant technology has thus gained the highest technological readiness level (TRL) among the emerging "green" monopropellants, it is still being evaluated in R&D programs, such as the European Horizon 2020 [19–23], US "green" propulsion evaluation programs [15], and before that the European FP7 Green Advanced Space Propulsion (GRASP) program in which the corresponding author too had actively contributed to the information generated by the program [18].

Whereas for monopropellant systems there already is some space heritage with the ECAPS "green" propulsion system, or RHP, which is comparable to existing

Figure 1.
Offek satellite top plate with monopropellant hydrazine thrusters [2].

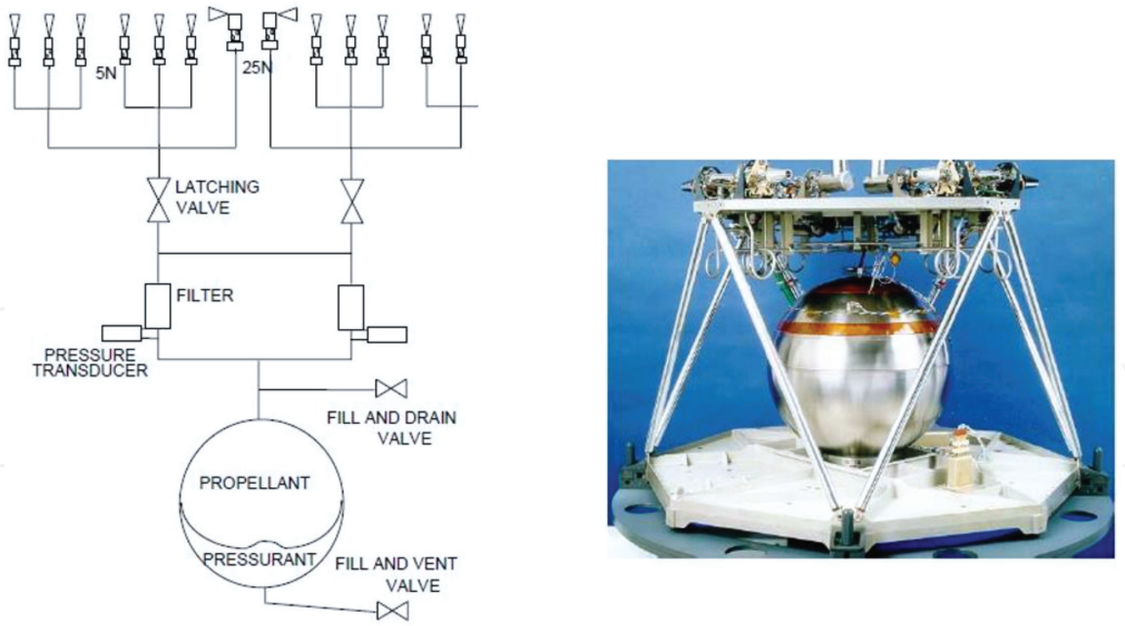

Figure 2.
The hydrazine propulsion module [3].

hydrazine-based systems, then for bipropellants, having higher specific impulse *Isp* and density impulse *ρIsp*, the situation is less advanced. Recently, an innovative hypergolic system, based on kerosene and hydrogen peroxide, has been developed by NewRocket© [24], which is similar in performance to MMH/N_2O_4. The NewRocket Green Propellant (NRGP) hypergolic bipropellant is based on concentrated hydrogen peroxide as oxidizer and on a kerosene-based fuel. NRGP has been made robustly hypergolic by addition of a minute amount of a solid energetic activator to the fuel, which is maintained homogeneously distributed in the fuel by its suitable gelation to a shear-thinning yield-stress fluid. This, while neat HTP and kerosene are not hypergolic. The shear-thinning feature of the fuel enables its full functionality in propulsion systems, including pressurized or pumped feed flow and injection to the reaction chamber, just like any liquid propellant.

Figure 3 depicts a bipropellant module schematic that is identical to the comparable MMH/N_2O_4 systems, with the regular components. The thruster assembly consists of a thrust chamber assembly (TCA) with injector, combustion chamber, and converging-diverging nozzle, as well as flow control valve (FCV) that controls fuel and oxidizer feeds. These feeds are provided by regulated pressure from their storage via dedicated manifolds with necessary valves, such as check valves, or inline valves that can be of various types: shape memory alloy actuators (SMA), pyrotechnical valves, or bistable latching valves (LV). The system feed and pressurization are serviced via fill and drain valves (FDV) and fill and vent valve (FVV). **Figure 3** also depicts the bipropellant firing test setup which has been realized at the Technion for various NRGP proof-of-concept and development model thruster systems.

Section 2 describes the proposed concept of gradual migration from monopropellant hydrazine propulsion systems to equivalent RHP systems. The concept is based on dual capability of an entire monopropellant chemical space propulsion system. Details are presented of the actual risk reduction program that has been employed for satellite hydrazine propulsion systems that may function also as "green" satellite propulsion systems employing an ADN-based RHP system. Concluding remarks are presented including a conceived way forward with an outlined proof-of-concept firing program [23].

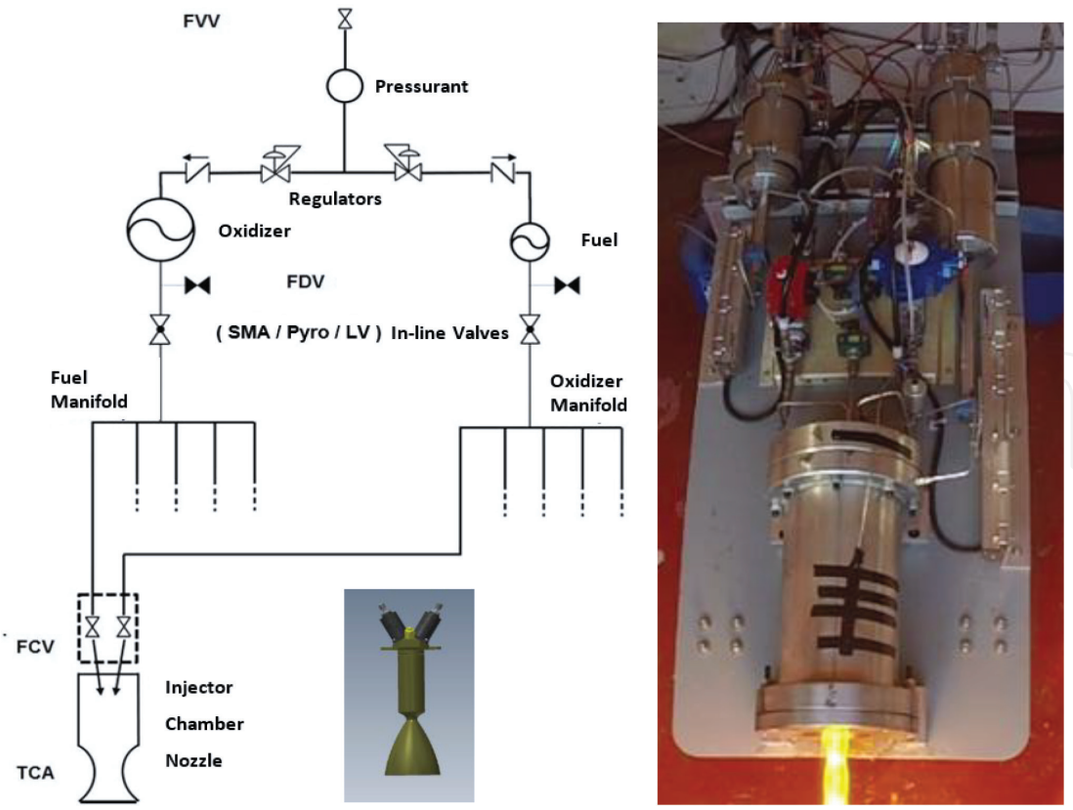

Figure 3.
The bipropellant module schematic (left) and test firing setup (right).

In Section 3, a similar comparable attitude is proposed for the hypergolic system based on kerosene and hydrogen peroxide, similar in performance to MMH/N_2O_4. Results are presented of the firing tests of the proof-of-concept and development model systems and of the NRGP fuel rheological characterization. The results of various engine types demonstrate the capability to operate this technology in both pulse and steady modes and in various thrust levels. This bipropellant technology offers a promising alternative to the presently employed hydrazine-based systems, through the fact that the fuel and oxidizer show very robust hypergolicity and short ignition delays, as well as characteristic velocity efficiency (ηC^*) exceeding 98%.

2. Dual capability monopropellant propulsion system

2.1 Overview

The concept presented is of gradual migration to equivalent RHP, or "green propulsion" systems. The proposed gradual conversion of monopropellant systems to RHP is by dual capability of entire conventional hydrazine systems to operate with ADN-based RHP, if so decided even just before the propellant loading. Namely, the suggested concept is of a propulsion system that may accept last moment decision on fueling with either hydrazine or with an RHP. This flexibility will enable the project to progress until a very late stage without necessary commitment to either one of the propellants, thus allowing a smooth transfer to RHP [23].

The hereby presented concept proposes to go a significant step further than the European "green" Myriade program, which has already sought components compatible both with hydrazine and ADN-based "green" monopropellant, with

the notable exception of the thruster assemblies, which will in their case have to be the special ECAPS thrusters [25]. In the "green" Myriade bus, the existing 230 mm propellant tank could be replaced with the one that has a silica-free diaphragm and flown successfully for over 5 years aboard the Swedish Prisma satellite with an ADN-based "green" propellant. For increased propellant capacity, existing larger tanks, using the same materials, can be used. These tanks are also compatible with hydrazine, as has been proven for the diaphragm material for long-term service aboard constellations such as Galileo-IOV and Globalstar-2 that are propelled by hydrazine [26, 27].

The ECAPS dual-mode thrusters and system employ their special thrusters as described in their patent of a thruster and a propulsion system that can be operated either in monopropellant mode or in bipropellant mode [28], as well as their new LMP-103S #1127-3 propellant variant [29]. It combusts at lower temperature giving a specific impulse (*Isp*), thus comparable with hydrazine, and it is stated that the lower combustion temperature may enable the usage of less expensive materials for the thrust chamber assembly (TCA). This last point is further elaborated in the paragraph below, detailing the risk reduction program of the dual capability monopropellant system, with a concept that has rather drawn some inspiration from the multifuel engine of the Reo trucks, which have had quite a widespread military use [30].

2.2 Risk reduction program

The initial risk reduction program that has been carried out is described here. It includes proof of concept of dual capability of all propulsion system parts and components, such as thrusters, valves, diaphragm tanks, pressure transducers, filters, and pipework. Materials' compatibility and operational use have been taken into consideration for both hydrazine and RHP, in view of a proposed system end-to-end proof by firing testing in space environment. The program was carried out by analysis of data as well as dedicated tests.

In the subparagraphs to follow, a number of areas are described, for which steps have been taken to reduce development risks. For most components, the materials compatibility is the main issue. This means that the effect of the propellant on the components must not be harmful, and on the other hand, the effect of the components' materials of construction shall not degrade the propellant itself.

Thereafter, functional issues are treated. The chemical reaction that converts the liquid propellant to the necessary high-energy gases takes place in the thrust chamber assembly (TCA) of the thruster. The catalytic effect on the ADN-based propellant has been proven with the same catalyst as in the hydrazine thruster.

The temperature of the high-energy gases, using the basic ADN-based propellant, is higher than is normally tolerated by the materials of construction of the hydrazine thruster's TCA. This issue is dealt with in a dedicated paragraph below.

The temperature necessary for inducing the nominal decomposition and oxidation reactions for ADN-based propellant is considerably higher than the 120–180°C necessary for hydrazine nominal decomposition. The tests that have shown the capability to achieve the necessary higher preheating of ADN-based propellant are described in the last subparagraph below.

2.3 Compatibility with ADN-based liquid propellants of COTS hydrazine systems' parts, components, and materials

The possibility to use commercial off-the-shelf (COTS) construction materials, which are used in typical hydrazine propulsion system components (tubing, valves,

filters, etc.), increases the flexibility, improves the reliability, and reduces the costs for introducing the ADN-based reduced hazards' propellants technology on future missions. FOI and ECAPS, who promote the ADN-based RHP FLP-106 and LMP-103S, respectively, have confirmed that most components can be COTS hydrazine propulsion system components [31, 32].

The materials, typically utilized for hydrazine propulsion systems, have been verified to be compatible with ADN-based liquid propellants and specifically with the LMP-103S space-proven aboard the Prisma satellite that was launched in June 2010 and operated successfully in space for 5 years. **Table 1** (based on Ref. [33]) presents these for the Prisma satellite.

In the present work, this concept is extended beyond previous works [23], to include also COTS monopropellant hydrazine thrusters, as described below.

2.4 Dual capability catalytic effect with ADN-based propellants

The catalytic effect on the ADN-based propellant has been proven with the same catalyst as in the hydrazine thruster. In the TCA, in which the chemical reaction converts the liquid propellant to the necessary high energy gases, there is need for a catalyst to induce such an ignition reaction. In laboratory thermochemical tests, it has been proven that the same iridium catalyst, which decomposes hydrazine, has a definite catalytic effect on the ADN-based propellant.

Differential scanning calorimetry (DSC) analysis has revealed an exothermal peak around 150°C in addition to the endothermic peak around 85°C of ADN melting and the thermal decomposition at 190°C. The peak around 150°C is attributable to the catalytic effect of heated iridium-based catalyst, which does not appear at low temperatures [34]. This has also been found in previously published works [35–38]. Ignition tests with DSC analysis, such as depicted in **Figure 4**, demonstrate this effect.

2.5 Temperature and water content effects

The temperature of the high-energy gases in the TCA, using the basic ADN-based propellant, is higher than is normally tolerated by the standard hydrazine thrusters. In order to overcome this limitation, the ADN-based propellants can be adjusted so that the catalytic effect is maintained, whereas the reaction temperature is reduced in order to have the TCA materials of construction within their required temperature limits. For dual use thruster application, this issue can be tackled by (a) using suitable TCA materials with compatibility to higher temperatures and (b) lowering the gas temperature. A combination of both is also possible.

Even though using TCA materials suitable for higher temperatures is not dealt with here, it is notable that these would also be suitable for the lower temperature

Component	Supplier	Status
Propellant tank	Rafael	Delta-qual by Rafael
Service valves	Moog	Qualified
Pressure transducer	Bradford	Qualified
System filter	Sofrance	Delta-qual by Sofrance
Latch valve	Moog	Qualified
Thruster	ECAPS	Qualified by ECAPS
Pipes and brackets	ECAPS/SSC	Qualified on STM

Table 1.
COTS parts and components flown in the Prisma satellite [33].

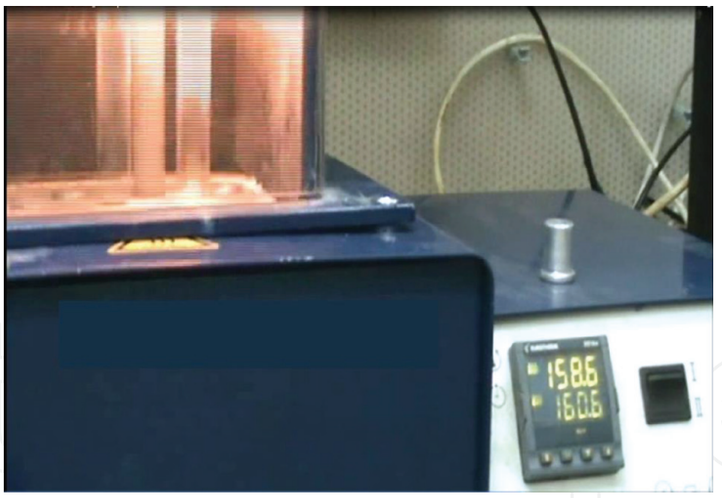

Figure 4.
ADN-based liquid monopropellant catalytic decomposition [34].

hydrazine decomposition products, which are the chemically nonoxidizing N_2, H_2, and NH_3.

As regards lowering the gas temperature, ECAPS presented their new LMP-103S #1127-3 propellant variant that also combusts at a lower temperature, giving a specific impulse comparable with the *Isp* for hydrazine. They stated that the lower combustion temperature may enable the usage of less expensive materials for the TCA [29]. For their low temperature derivative of LMP-103S, which ECAPS have recently developed, they have conducted hot-firing tests at their facility at FOI-Grindsjön [29, 39], as well as in cooperation with Airbus Safran Launchers (ASL) in the facility at DLR-Lampoldshausen [23, 40–43]. Although the declared intention of the ECAPS development was to handle significantly lower storage temperatures than specified for traditional storable monopropellants, for example, hydrazine (down to about −30°C), this propellant also exhibited a lower combustion temperature than LMP-103S, giving a specific impulse comparable with the *Isp* for hydrazine. The low-temperature derivative of the space-qualified LMP-103S was tested in a 22N development thruster, having 20% higher density than hydrazine, combusting at a lower temperature than LMP-103S and with *Isp* similar to hydrazine [29].

Lowering TCA gas temperatures by the effect of further dilution in water of established ADN-based propellants is expected to be in line with the reduction of the energetic content of the decomposition products. This leads directly to reduction in the temperature of the decomposition gases. The desired effect achieved by this is the possibility to use less demanding materials of construction, but with lower performance. Thruster performance is linked to the temperature directly, as follows. The specific impulse is proportional to the square root of the ratio between temperature and molecular weight of the exhaust gas, or $Isp \sim \sqrt{Tc/M}$ [44]. Therefore, as expected, specific impulse is reduced too, per the square root of temperature.

The specific impulse relation to temperature, $Isp \sim \sqrt{Tc/M}$, is similarly applicable to comparing hydrazine and the ADN-based monopropellant FLP-106 [8]. The specific impulse of FLP-106, as shown in **Table 2**, is higher than that of hydrazine, in accordance with its considerably higher chamber temperature.

A detailed investigation and analysis on the influence of the water content on the specific impulse and the thermochemical and density properties of the propellant has been presented in a recent conference by GRASP FP7 group participants. They presented the influence of water content on the ignition process and the spray behavior and the influence on the thermal field inside the combustion. The analysis of the spray behavior in vacuum near conditions was investigated by using different

Monopropellant			Hydrazine	FLP-106
Density	ρ	g/cm^3	1.0037	1.357
Specific impulse based on mass flow	*Isp*	s	230	259
Specific impulse based on volume flow	ρIsp	s g/cm^3	231	351
Chamber temperature	*Tc*	°C	1120	1880

All properties at 25°C, Isp calculated for reaction chamber pressure Pc = 2.0 MPa, ambient pressure Pa = 0.0 MPa, expansion ratio ε = 50.

Table 2.
Comparison of the properties of the monopropellants hydrazine and the ADN-based FLP-106 [8].

blends. For the analysis of the combustion chamber temperatures, the temperatures and the heat flux inside the combustion chamber in relation to the water content were estimated [45], as well as the impact of the water content and the results for a 500N class thruster.

The following results were obtained in Ref. [45]. Expansion ratio ε = 50 and chamber pressure Pc = 20 bars were assumed, and the reaction was feasible in the investigated concentrations in water, according to the calculations made. The density reduction still leaves the blend with a considerably higher density than hydrazine, with the corresponding gain in density-specific impulse ρIsp, decreasing to the lowest value of 280 kg s/L. This is nevertheless approximately 22% higher than the value calculated for hydrazine. Blends bringing *Isp* down to values similar to those of hydrazine are considered. Density and ρIsp as a function of temperature for water and FLP-106 at various degrees of water content are presented in **Figure 5** (from Ref. [45]).

2.6 Preheating temperature capability

The dedicated ADN-based thrusters are ignited with a preheated catalyst. The ECAPS 1N thrusters, specifically developed for ADN-based monopropellant, use a 10 W heater. The preheating time is 1800 s. In the case of the Prisma thruster, the maximum load during preheating was 9.25 and 8.3 W during firing [46].

The necessary preheat temperature for inducing the reaction of ADN-based propellant is considerably higher than the 120–180°C of hydrazine decomposition. For nominal performance, the required preheat temperatures were in the order of 200–300°C [33]. FLP-106 was experimentally ignited thermally and by resistive heating, within less than 2 ms. An optimal preheating temperature of about 300°C was found where the ignition delay was minimized [47].

Preheating tests have been carried out with a conventional 1N monopropellant hydrazine thruster, with nominal electrical supply voltage in a vacuum chamber that simulates space conditions. These have shown the capability to achieve with a conventional hydrazine thruster the necessary higher preheating of ADN-based propellant, as depicted in **Figure 6** [34]. This heating period compares well with the abovementioned 1800 s of the Prisma satellite in-orbit performance.

2.7 Proof-of-concept firing program

After removing, within the described initial risk reduction program, the major uncertainties regarding the proposed dual capability of monopropellant hydrazine propulsion systems to operate as equivalent reduced hazards propellant (RHP) systems, a proof-of-concept firing program has been proposed. This program entails end-to-end proof by firing testing in simulated space environment of a representative engineering model (EM) propulsion system.

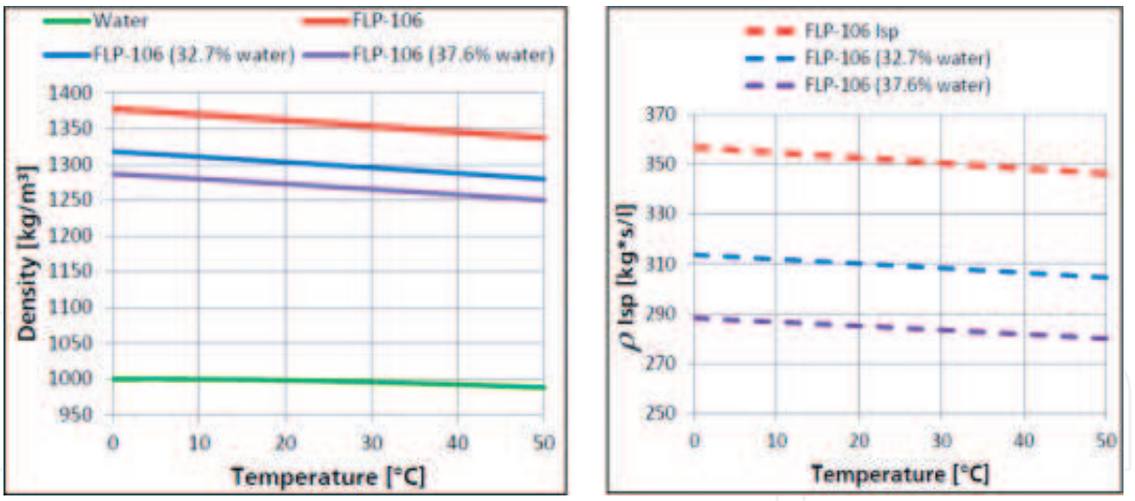

Figure 5.
Density and ρIsp as a function of temperature for water and FLP-106 with various values of water content [45].

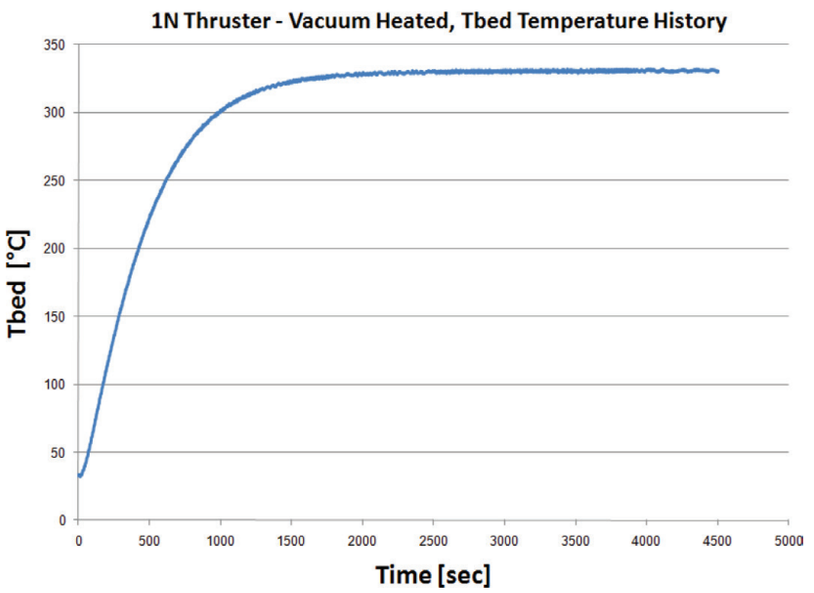

Figure 6.
1N thruster catalyst bed temperature preheat in simulated space conditions [34].

The proposed test setup is based on existing hydrazine propulsion systems vacuum chamber infrastructure adaptation to ADN-based monopropellant firing, without long-term interference with the capability to continue with hydrazine system tests. The test chamber is the one previously used for the Offek satellite EM firing and depicted in **Figure 7** [1].

The difference between the propellants requires attention to aspects of quality and safety to personnel, as well as to those of the testing infrastructure. Primarily, the ADN-based propellant, which is an oxidizer by nature, needs to be very strictly separated from hydrazine, which is fuel by nature. This can be achieved by temporarily disconnecting the existing hydrazine feed lines from the vacuum test chamber setup and maintaining the necessary separation distances according to the materials involved and their quantities. Moreover, the vacuum pump lines should be equally separated, in order to prevent any concern regarding carried over propellants' traces being in contact with each other.

A location independent feed system has been designed for the ADN-based "green" monopropellant, which would be entirely enclosed within the testing

vacuum chamber (**Figure 7**). This is consistent with the end-to-end testing of the entire system, as was done with the hydrazine system EM firing tests.

Here, the handling procedures can be simplified, thanks to the reduced hazards involved with the handling of RHP. The Prisma satellite fueling campaign serves as an example for that, as illustrated in **Figure 8**. During the launch campaign of the Prisma satellite, the first in-space demonstration of an ADN-based propulsion system, ECAPS loaded the hydrazine and RHP propellants at the Yasny launch base. The handling of ADN-based RHP was evaluated and declared as a "nonhazardous operation" by the Range Safety, so SCAPE suits were not required during the Prisma ADN-based propellant loading operation [20, 48].

The firing program, like any new type of testing, needs to go through the common procedural requirements. These include safety reviews and safety approvals, test procedure preparation and approval, allocation of thruster and propellant, and allocation of the test facility. The procedural requirements have been fulfilled, with the exception of the facility allocation.

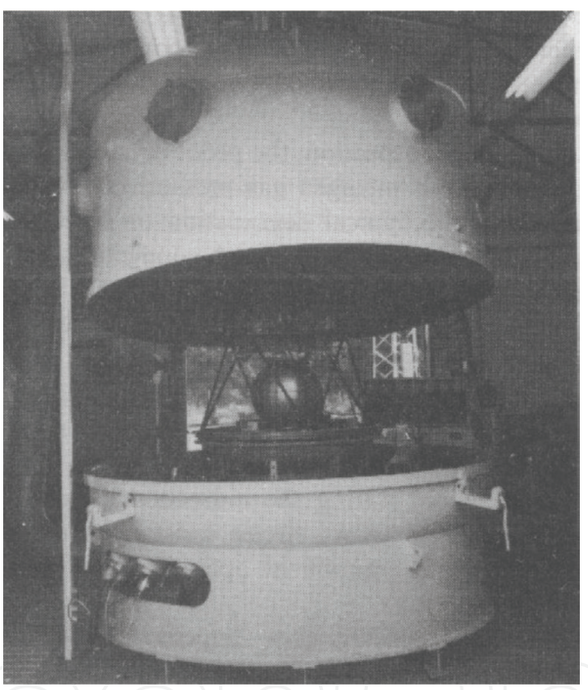

Figure 7.
Entire system EM testing vacuum chamber [1].

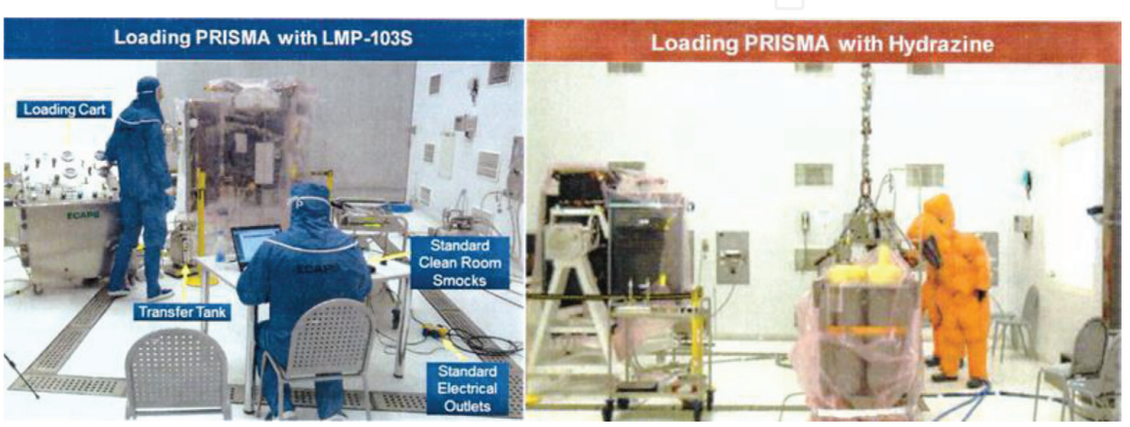

Figure 8.
Propellant loading of satellite Prisma [20].

2.8 Concluding remarks for monopropellant

An initial risk reduction program has been performed for the concept of dual-capability propulsion systems. This was done by analysis of data as well as by dedicated tests. The program included proof of concept of dual use of all propulsion system parts and components, such as thrusters, valves, diaphragm tanks, pressure transducers, and pipework. The dual use of the propulsion systems' key components, the thrusters, is beyond any previous work. Both material compatibility and actual operation have been justified for both hydrazine and RHP, in view of an eventual system end-to-end proof by firing testing in space simulation environment.

The concept of dual-capability systems may serve as a vehicle toward gradual migration from monopropellant hydrazine propulsion systems to equivalent RHP systems. Hydrazine systems are prevalent in several applications and are still often the systems of choice in space propulsion as well as in other applications. The slow introduction rate of RHP or "green propellants," into space systems due to the conservatism of the space propulsion industry may be expedited thanks to the possibility for gradual conversion by dual capability of conventional hydrazine systems and ADN-based RHP. The presented propulsion system concept may accept last moment decisions on fueling with either hydrazine or with an RHP. This flexibility enables project progress until a very late stage without necessary commitment to either of the propellants, thus allowing a smoother transfer from hydrazine to RHP.

3. Comparable bipropellant rocket propulsion system

3.1 Overview

This section describes a hypergolic system based on kerosene and hydrogen peroxide, similar in performance to MMH/N_2O_4 that has been developed by NewRocket© [24]. The NewRocket Green Propellant (NRGP) hypergolic bipropellant is based on concentrated hydrogen peroxide (HTP—high test peroxide) as oxidizer and on a kerosene-based fuel. NRGP is used in a family of bipropellant rocket and gas-generator applications. Neat HTP and kerosene are not hypergolic, while NRGP has been made such by addition of a minute amount of a solid energetic activator to the fuel. The activator is maintained homogeneously distributed in the fuel by its suitable gelation to a shear-thinning yield-stress fluid. Shear-thinning fluids exhibit decreased viscosity with increasing applied shear stresses, such as by pressure gradients (ΔP). The shear-thinning feature of the fuel enables its full functionality in propulsion systems, including pressurized or pumped feed flow and injection to the reaction chamber, just like any liquid propellant.

Usually, decomposition of hydrogen peroxide is achieved using catalyst beds based on silver, platinum, and other materials. Catalyst beds produce high-temperature-decomposed hydrogen peroxide that can burn with a hydrocarbon fuel; however, the system complexity and weight are both increased.

Another method is based on the idea of using catalytic or reactive material (such as metal oxides—MnO_2, PbO_2, F_2O_3, etc.) that is dissolved in a liquid fuel. The reactive material decomposes hydrogen peroxide and ignites the fuel, so hypergolic ignition is achieved without the use of a catalyst bed. However, this method requires fuels such as ethanol or methanol that serve as solvents for the reactive material. All these solvents used either alone or with kerosene-based fuels and have relatively low heat of combustion; therefore, the energetic performance of the system is low.

By nature, hydrogen peroxide and kerosene do not ignite upon contact. However, in a gelled fuel, the existence of yield stress assures that particles (reactive or catalytic) can be added without the effect of sedimentation or buoyancy. Gels enable the suspension of reactive or catalyst particles, uniformly distributed in the fuel, without compromising the energetic performance of the system. The use of suspended particles enables a quite large variety of combinations of fuels and oxidizers that can become hypergolic by gelling one of the liquids and adding the proper material.

Natan et al. [49] came up with the idea of embedding reactive particles with hydrogen peroxide in gelled kerosene. Drop-on-drop tests exhibited that this kind of gelled kerosene is hypergolic with hydrogen peroxide as shown in a sequence of photographs in **Figure 9**. Total ignition delay time was 8 ms. Connell et al. [50–52] also investigated the issue and showed that it is feasible.

The idea was adopted by a start-up company, NewRocket that proceeded with the development of a prototype motor using gelled kerosene with reactive particles and hydrogen peroxide [24]. **Table 3** shows the characteristics of their NRGP propellant in comparison to other candidate propellants.

Here again the specific impulse relation to temperature, $Isp \sim \sqrt{Tc/M}$, is applicable to comparing MMH/N_2O_4 and the kerosene and hydrogen peroxide-based green bipropellant NRGP. The specific impulse *Isp* of NRGP, as shown in **Table 4**, is some 4% lower than that of MMH/N_2O_4, in accordance with its considerably lower chamber temperature; but it is noteworthy that its ρIsp is higher by 4% thanks to its 8% higher average density.

Experiments have been conducted in a lab-scale motor to verify the feasibility of the idea. The main problems were the atomizers because the particles initially caused plugging of the exit. The problem was solved by changing the type of reactive particles and by increasing the atomizer diameter. The system (**Figure 10**) was found to operate properly, and by using adequate valves, operation in pulses was achieved as shown in **Figure 11**.

In the next sections, the stability of the fuel for no phase separation or sedimentation throughout its life cycle is demonstrated by theoretical and experimental considerations.

3.2 Yield stress fluids

The NewRocket Green Propellant (NRGP) gelled fuel has been classified as a yield-stress fluid, and this feature has been demonstrated and quantified by tests that included rheological characterization, application of dynamic environment such as acceleration in centrifuge, and real-time storage and handling. The following paragraphs elaborate on that, while being extensively based on Spicer and Gilchrist [53], and are included here in order to make the present chapter quite self-contained.

Yield-stress fluids have the feature of solid-like materials in that they do not flow until a critical stress ($\boldsymbol{\sigma}_y$) is exceeded, after which they flow like a liquid. Modeling such behavior often begins with a nonzero value of the yield stress term $\boldsymbol{\sigma_y}$ in the Herschel-Bulkley-Extended (HBE) equation.

$$\boldsymbol{\sigma} = \boldsymbol{\sigma_y} + \boldsymbol{k}\dot{\boldsymbol{\gamma}}^{\boldsymbol{n}} + \boldsymbol{\mu}_\infty \dot{\boldsymbol{\gamma}} \tag{1}$$

Here $\boldsymbol{\sigma}$ is the stress applied on the fluid, $\dot{\gamma}$ is the shear rate, $\boldsymbol{k}$ is a proportionality constant termed the consistency coefficient (viscosity at $\dot{\gamma} = 1$), **n** is a power law exponent termed the flow index, and μ_∞ is the constant viscosity in the very high shear rate range.

Eq. (1) is able to describe power law behavior and includes the additional yield stress term $\boldsymbol{\sigma_y}$. Yield-stress fluids are typically shear thinning and have an exponent of $\mathbf{n} < 1$.

The expectation that a fluid might have a yield stress comes from an understanding of the fluid microstructure and its relevant length and time scales. Generally, attractive interactions between colloids, physical crowding of larger particles, and cross-links between polymers or micelles can all provide a finite yield stress to a fluid. Concentration is also a key variable in yield-stress fluids. Very dilute suspensions can have a yield stress but only if the particles attract each other strongly such that they stick together upon collision. The rheology of a suspension gel is highly dependent on whether the particles attract one another strongly enough to form a network that resists flow. Gel microstructure is often a unique function of its

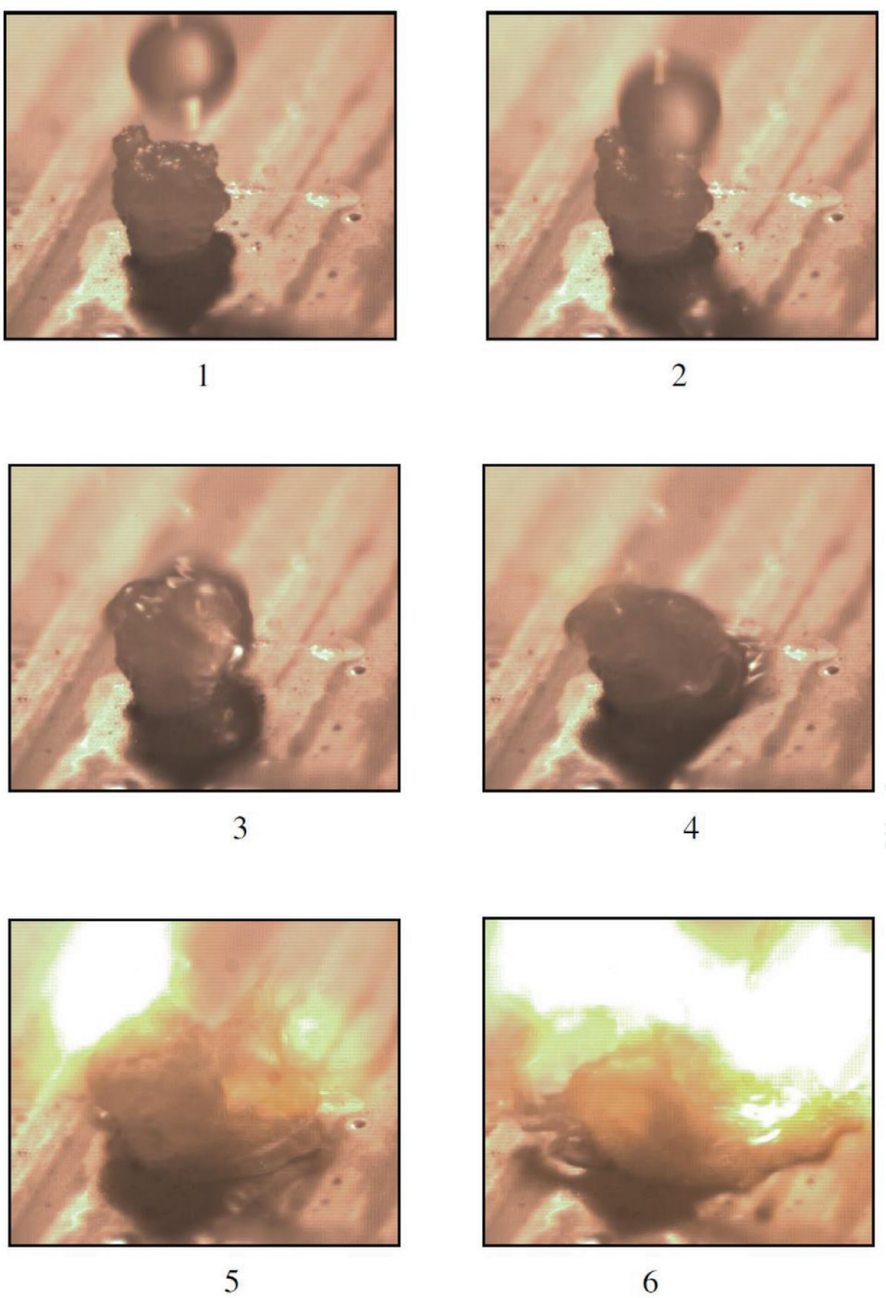

Figure 9.
A sequence of high-speed photographs demonstrating hypergolic ignition of hydrogen peroxide with kerosene. The time interval between sequent pictures is 2 ms [24].

Propellant	Toxicity	Storability	Cost	Safety	In flight control	Hypergolic ignition
Solid	Low	High	Low	Medium	No	No
Hybrid	Low–none	High	Medium	Medium–high	Yes	No
Hydrazine	High	High	High	Low	Yes	Yes
Ionic propellants ADN-based (HPGP-LMP-103S*)	Low	Medium–high	Medium–high	Medium	Yes	Yes
Bipropellants NTO/MMH*	High	High	High	Medium	Yes	Yes
Electric ion thrusters arcjet	None	High	High	Medium	Yes	_
NRGP	None	High	Low	High	Yes	Yes

Table 3.
Characteristics of candidate propellants [24].

Bipropellant			MMH/N_2O_4	NRGP
Average density	ρ	kg/L	1.2	1.3
Specific impulse based on mass flow	*Isp*	s	341	328
Specific impulse based on volume flow	ρIsp	s kg/L	409	426
Chamber temperature	*Tc*	°C	3125	2580

All properties at 25°C, Isp calculated for reaction chamber pressure Pc = 2.0 MPa, ambient pressure Pa = 0.0 MPa, expansion ratio ε = 50.

Table 4.
Comparison of the properties of the bipropellant composition MMH/N_2O_4 vs. NRGP with kerosene-based fuel/H_2O_2.

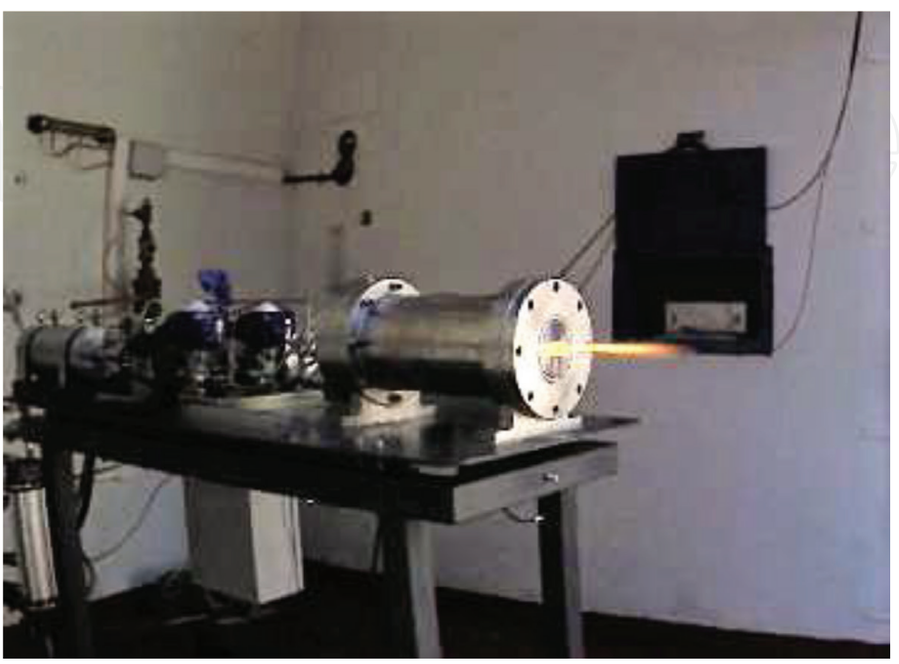

Figure 10.
NewRocket lab-scale experimental system.

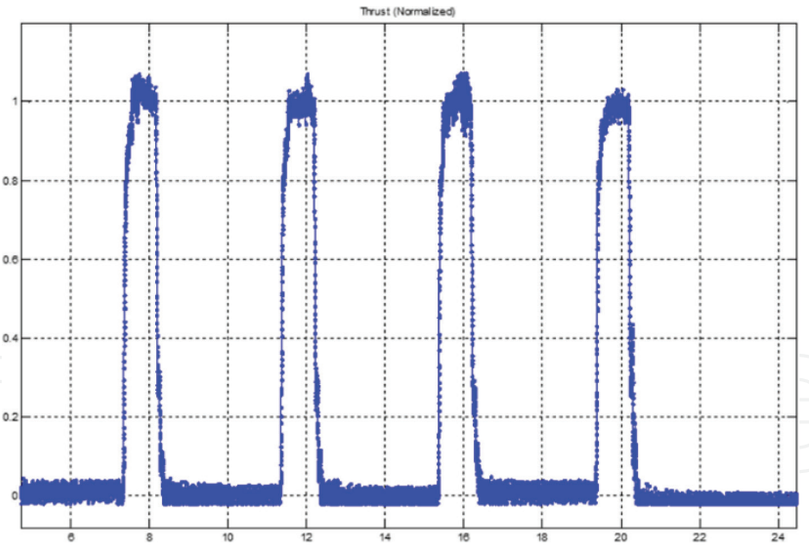

Figure 11.
NewRocket engine operation in pulses.

processing history because the particle networks can grow, break, and reform under flow.

3.3 Yield-stress suspension of particles vs. Stokes law settling

The ability of the NRGP fuel, as a yield-stress suspension, to suspend solid particles in the gelled kerosene without any displacement occurring until a shear stress of $\boldsymbol{\sigma_y}$ or above is applied, is of key importance. For that, an estimate is made of the magnitude of yield stress required to suspend a given particle. It is important to contrast this treatment with the following Stokes law description of particle settling in a Newtonian fluid, derived via a force balance between the buoyant and drag forces acting on a suspended particle:

$$v = \frac{(\rho_p - \rho_l)\, d^2 g}{18\mu} \tag{2}$$

where the sedimentation velocity at low Reynolds numbers, **v**, is a function of the particle $\boldsymbol{\rho_p}$ and liquid $\boldsymbol{\rho_l}$ densities, the particle diameter **d**, gravitational acceleration ***g***, and the fluid viscosity **μ**. For other than gravitational accelerations, ***g*** would be replaced by the applicable acceleration ***a***.

Rearranging Eq. (2) to solve for viscosity and substituting the height to shelf life ratio for velocity obtains Eq. (3), with sedimentation length and time, **h** and **t**, respectively instead of velocity **v**.

$$\mu = \frac{(\rho_p - \rho_l)\, d^2 g t}{18h} \tag{3}$$

The performance of viscosity with that of a yield stress for the same application can numerically be contrasted by day by day examples [53]. A fluid with a yield stress not exceeded by the acceleration stress of a particle is not described by Eq. (2) because it essentially possesses an infinite viscosity at low stresses and no flow can occur. By taking the ratio of the particle gravitational stress to the fluid yield stress and assuming a hemispherical characteristic area of the yield surface formed, a dimensionless parameter, **Y**, is obtained to be used to calculate whether a particle will sediment in a yield-stress fluid:

$$\mathbf{Y} = \frac{2\pi\left(\frac{\mathbf{d}}{2}\right)^2 \boldsymbol{\sigma}_y}{\frac{4}{3}\pi\left(\frac{\mathbf{d}}{2}\right)^3 (\boldsymbol{\rho}_p - \boldsymbol{\rho}_l)\boldsymbol{g}} = \frac{3\boldsymbol{\sigma}_y}{\mathbf{d}(\boldsymbol{\rho}_p - \boldsymbol{\rho}_l)\boldsymbol{g}} \quad (4)$$

where $\mathbf{d}$ is the particle radius and $\boldsymbol{\sigma}_y$ is the fluid yield stress. It is worthwhile noting that the critical $\mathbf{Y}$, $\mathbf{Y}_{crit}$, bounding the states of suspension and sedimentation, is less than unity because of the finite fluid volume yielded by the particle. This means that the yield stress required to suspend a given particle is actually less than the gravitational stress the particle exerts. Simulations give a value of $\mathbf{Y}_{crit} = 0.14$ [54], while experiments produce $\mathbf{Y}_{crit}$ values between 0.1 and 0.6 [55]. Since the critical criterion can vary significantly, so can the suspension efficiency of a yield-stress fluid. Eq. (4) can be used to estimate the yield stress required to stably suspend a small solid particle by assuming a worst case of a $\mathbf{Y}_{crit} = 1$. If the worst case application is not satisfying the requirements, then Eq. (4) may be used to remove the extraconservatism by using it as a nondimensional index. This can be experimentally determined for a specific fluid-particle system using a test in which the suspension stability of a range of particle sizes or densities is recorded for a specified yield-stress fluid and the transition from stability to sedimentation is recorded. The approach described above applies to sedimentation of a dilute suspension of particles through a homogeneous yield stress fluid or, equivalently, of a much larger single particle through a homogeneous suspension of small particles.

It can be demonstrated [53] that yield stress can be a very efficient means of stabilizing particle suspensions because it can entirely prevent any particle motion, whereas viscosity merely slows particle motion.

3.4 Calculation of the sedimentation threshold acceleration of a particle through the NRGP gelled fuel

Rearranging Eq. (4) and replacing the gravitational acceleration $\boldsymbol{g}$ with the applicable acceleration $\boldsymbol{a}$ in order to solve it, and substituting the height to shelf life ratio for velocity, obtains Eq. (5).

$$\boldsymbol{a} = \frac{3\boldsymbol{\sigma}_y}{\mathbf{Y} \cdot \mathbf{d}(\boldsymbol{\rho}_p - \boldsymbol{\rho}_l)} \quad (5)$$

Using Eq. (5) for a particle with diameter $\mathbf{d} = 2$ μm and density of $\boldsymbol{\rho}_p = 1.45$ g/cc, immersed in a gel with density $\boldsymbol{\rho}_l = 0.8$ g/cc and with a $\boldsymbol{\sigma}_y$ of 10 Pa (a conservative order of magnitude representative of the 16 Pa measured in the paragraph below), while assuming a worst case of a $\mathbf{Y}_{crit} = 1$, the solid particle will start to move when the acceleration reaches a threshold value of $\boldsymbol{a} = 23{,}077$ m/s^2 or $\boldsymbol{a} = 2352\boldsymbol{g}$.

3.5 Calculation of the sedimentation velocity and distance of a particle through the NRGP gelled fuel

When the yield stress $\boldsymbol{\sigma}_y = 10$ Pa, which is the conservative threshold for movement, has been surpassed by applying acceleration 2400 g (in excess of 2352 g), the sediment movement velocity of a particle through fluids can be calculated using Eq. (2). Here the acceleration of gravity $\boldsymbol{g}$ would be replaced by the applicable acceleration $\boldsymbol{a}$.

$$v = \frac{(\rho_p - \rho_l)\, d^2 a}{18\mu} = \frac{650\frac{kg}{m^3} \cdot (2 \cdot 10^{-6} m)^2 \cdot (2400 \cdot 9.81) m/s^2}{18 \cdot 100\, Pa \cdot s} = 3.5 \cdot 10^{-9} m/s \quad (6)$$

This, with a gel viscosity measured in experiments of $\mu_g = 100\ Pa \cdot s$. However, the viscosity derived from the Herschel-Bulkley rheological model coefficients in the following paragraph would be taken into account here.

In 10 s under acceleration of 2400 *g*, the resultant sedimentation distance is 3.5×10^{-8} m, namely one-thirtieth of a micron sedimentation. In 10 years ($10 \times 3600 \times 24 \times 365 = 3.15 \times 10^8$ s), this represents sedimentation of 1 m, namely full sedimentation. Therefore, it is important to remember that the extremely high acceleration value, in the order of km/s^2, was assumed here just in order to compare to the actually high yield stress of the fuel, while in reality any considerable accelerations are applied on the fuel for very short periods only, such as experienced by space launch.

For a fuel with similar viscosity, but without a yield stress (not being the case here), for gravitational acceleration of 9.81 m/s^2, in 10 years the sedimentation would merely be 4 mm.

It can be seen that the sedimentation distance of a particle is proportional to its squared diameter, gravity, and particle density and inversely proportional to the viscosity of the gel. Thus, it is possible to reduce the sediment distance by the following ways: reducing particle diameter, reducing particle density, and increasing the viscosity of the gel.

Based on Technion experience, it can be stated that after storage of a couple of years, there is no degradation in terms of phase separation, sedimentation, agglomeration, ignition delays, etc. For quantitative evaluation of these behaviors, both real-time and accelerated tests are relevant. These were obtained by centrifuge tests for assessing the stability of the gel in accelerations.

To simulate the mechanical environmental loads during a typical rocket launch, which might cause concern regarding gel separation in the tank and propellant feed system, centrifuge tests have been conducted. Example of result obtained for a gelled fuel with a suspended particle with a diameter of 250 μm is depicted in **Figure 12**, which shows the gel stability as a function of operating time or degree of acceleration. In this experiment, a gelled fuel sample within a test tube was tested in a centrifuge for assessing the influence of two different conditions: firstly, applying constant acceleration (40 g) while varying the time duration (**Figure 12** left) on the test and secondly, applying constant duration time (2 minutes) while varying the magnitude of the acceleration (**Figure 12** middle). After each centrifuge test, the separated liquid due to the acceleration has been sought in order to be compared with the initial mass to quantify the stability of the investigated gel.

It is important to note that from a visual examination of all samples, no particle sedimentation was observed.

3.6 NRGP fuel rheological characterization

3.6.1 Measuring system

For characterization of the rheological behavior of the gelled fuels, a TA Instruments AR 2000 rotational rheometer [56] operated in controlled rate mode is being used. The rotational rheometer imposes strain to the liquid and measures the resulting stress for shear rates up to 1000 1/s. Most common test geometries

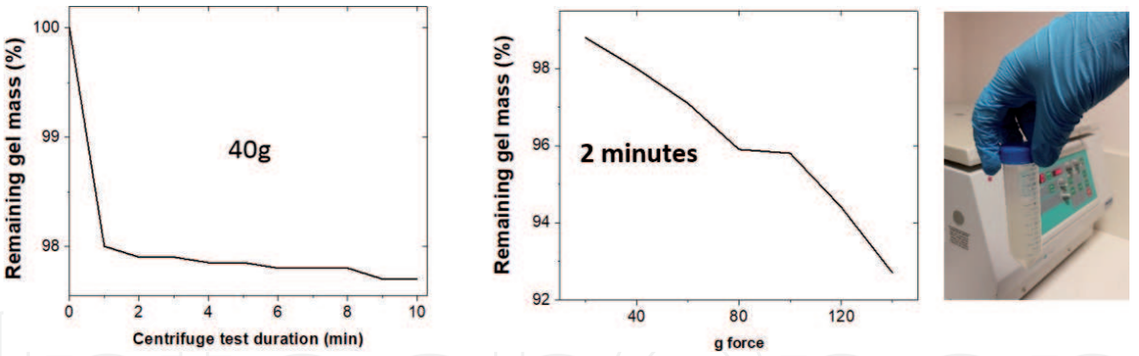

Figure 12.
Gel stability as a function of test duration time (left) and acceleration value (middle). On the right is a test tube before centrifuge test.

for rotational rheometers are the parallel plates (see **Figure 13** right) and the cone and plate. The parallel plates configuration has been used here for gel characterization. A Peltier plate-type temperature regulation system inside the equipment ensures the prescribed controlled fluid temperatures during rheological measurements.

3.6.2 NRGP measured results

For measuring shear-thinning and thixotropic characteristics, fuel gel samples were subjected to hysteresis loop tests starting with increasing shear rate $\dot{\gamma}$ from 1 to 100 s^{-1} (up curve) and then reducing back from 100 to 1 s^{-1} (down curve) while measuring the viscosity μ. In **Figure 14**, it can be seen that the shear-thinning behavior is significant: μ decreases almost two orders of magnitude in the presented shear rate range. At high shear rates $\dot{\gamma} > 10^2$ s^{-1} (not in the figure), the shear-thinning behavior diminishes due to the destruction of the gel structure and leads to a constant viscosity value μ_∞, which is called upper Newtonian plateau and its value is near the viscosity of the Newtonian neat fluid fuel.

This result is in accordance with the requirements for the rocket engine propellant feeding system, for which the gel fluid passes through a pipe and finally is injected into the combustion chamber. The injectors are small in both length and cross-sectional area, and the fluid remains there for a very short time. The shear rates developed in the injectors due to the sudden decrease in the cross-sectional area are very large, and the shear-thinning effect is dominating.

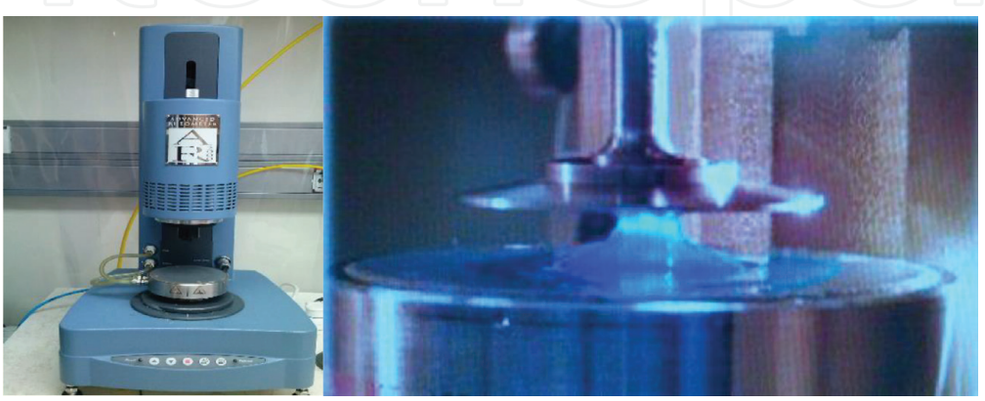

Figure 13.
AR 2000 rheometer and parallel plates [56].

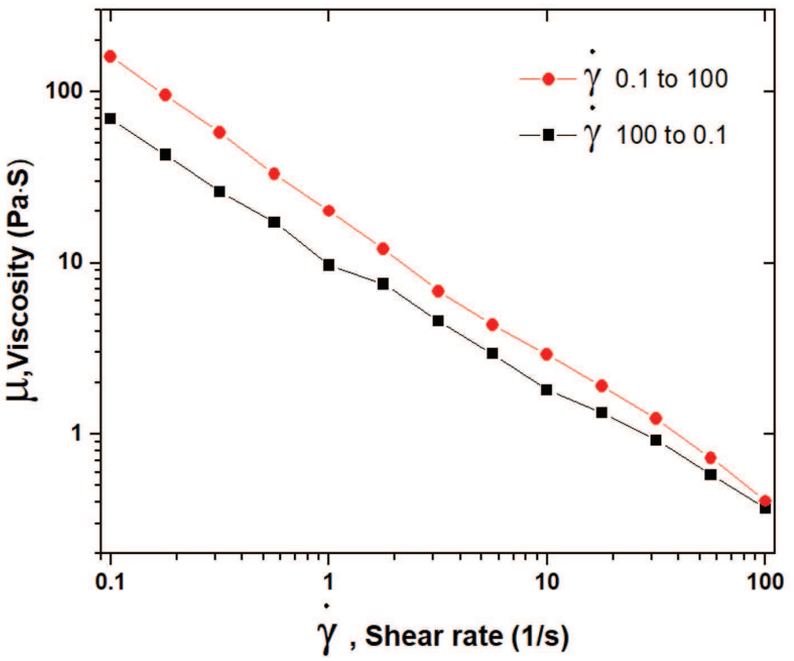

Figure 14.
Gelled fuel viscosity as a function of shear rate.

3.6.3 Yield stress measurement

The yield stress value of the gelled fuel can be measured by two main methods:

a. Shearing the fluid at a low and constant shear rate and measuring the shear stress as a function of time. In this method, the yield stress is defined as the maximal measured value as shown in **Figure 15a**.

b. Measuring the shear stress vs. shear rate and extrapolating to zero shear rate (**Figure 15b**) using the Herschel-Bulkley equation, as detailed above for Eq. (1).

Here method (b) was used for measuring yield stress on the rotational rheometer, that is, by extending the flow curve at low shear rates and taking the shear stress y-axis intercept as the yield value. Using this method for an NRGP fuel sample is shown in **Figure 16**. In this example, the measured yield stress value is 16 Pa.

The three aspects of the shear relevant rheological behaviors of a gel, that is, shear-thinning, upper Newtonian plateau, and yield stress, can be described by a constitutive equation, which is the Herschel-Bulkley extended (HBE) equation, Eq. (1), expressed here in terms of viscosity. This equation describes the dependence of the shear viscosity on the shear rate.

$$\mu = \frac{\tau_0}{\dot{\gamma}} + \mathbf{K} \cdot \dot{\gamma}^{\mathbf{n}-1} + \mu_\infty \tag{7}$$

As mentioned above, **n** is the flow behavior index that varies from "0" for very shear thinning materials to "1" for Newtonian materials. A smaller value of **n** means a greater degree of shear thinning. An example using HBE method for assessing the shear thinning behavior is shown in **Figure 17**.

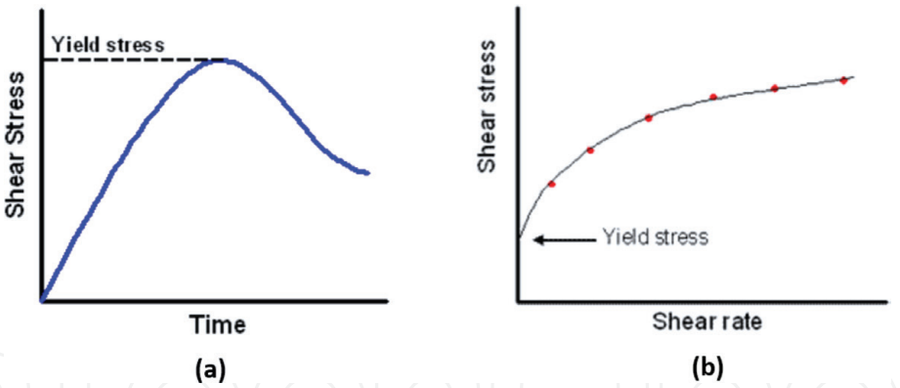

Figure 15.
Common methods for measuring yield stress [56]. (a) Shearing a fluid at a low and constant shear rate and measuring the shear stress as a function of time and (b) extending the shear stress vs. shear rate curve at low shear rates.

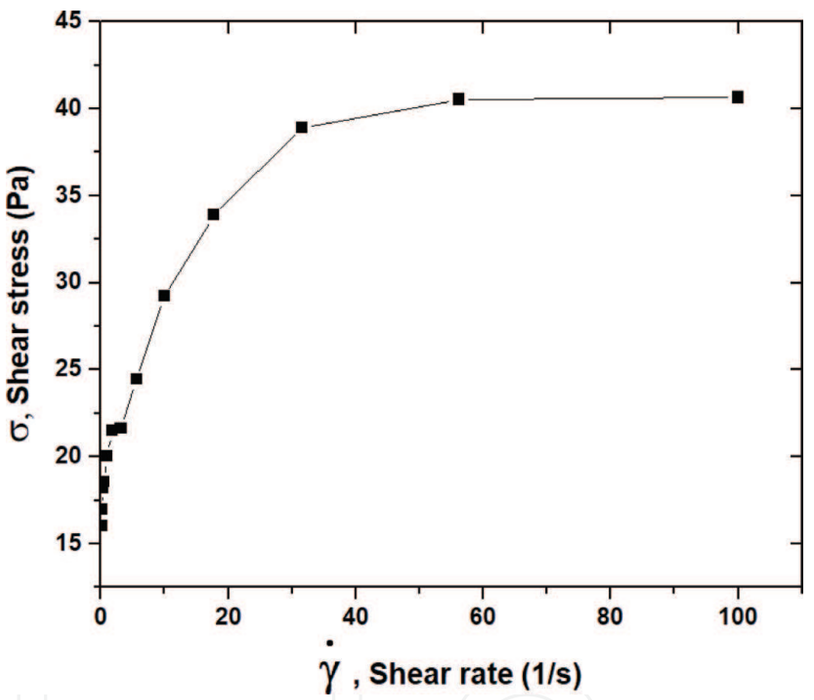

Figure 16.
Yield test for an NRGP fuel.

3.6.4 Temperature effect

The gel fuel temperature has an effect on its rheological properties (shear thinning, yield stress, thixotropic behavior). In general, the yield stress of the gel decreases with increasing temperature since the cohesion forces between the gel molecules are decreasing and their mobility is increasing, thereby the resistance of the gel to deformation is reduced as the temperature increases. Shear thinning and thixotropic behaviors are becoming less prominent at higher temperatures.

An example of measurement made for an NRGP fuel gel sample at three different temperatures, −10, +40, and +70°C is shown in **Figure 18**, which shows that the influence of the temperature on the viscosity values is more prominent at lower shear rates and the shear thinning behavior becomes less prominent as the temperature increases.

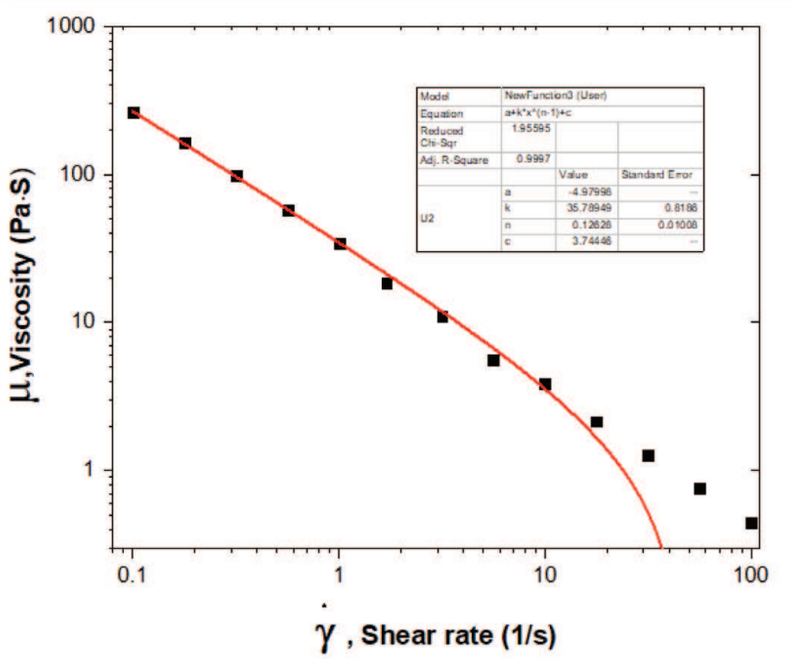

Figure 17.
Curve fitting using Herschel-Bulkley extended model.

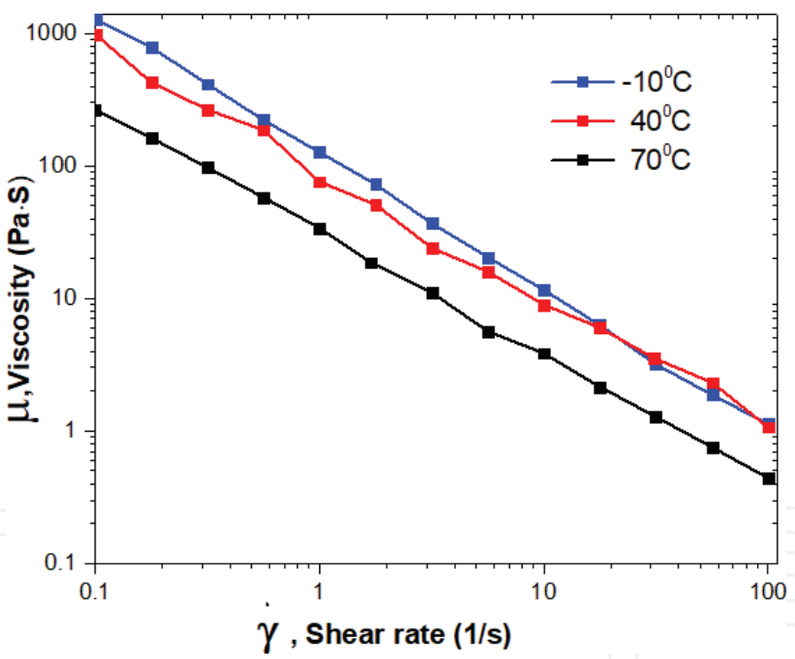

Figure 18.
Gelled fuel viscosity as a function of shear rate at −10, 40, and 70°C.

It is important to note that for an expected operational range of −10 to +40°C, the temperature effect is very small.

Visual inspection of a sample that has been exposed to a temperature of 80°C revealed no phase separation or sedimentation at all. Other changes (color, bubbles, pitting) were not observed either.

3.7 Concluding remarks for bipropellant

Recently, it has been recognized that "the development of a bipropellant gel propellant system, which is ideally both green and hypergolic, is an important area

of research" [57]. In general, the NewRocket concept seems to be such that can provide replacements for hydrazines in many types of applications, most notably as "green" replacement to the veteran bipropellants MMH and N_2O_4.

The results of the firing tests of the proof-of-concept and development model systems demonstrate the capability to operate this technology in both pulses and steady modes and in various thrust levels. This bipropellant technology offers a promising alternative to the presently employed hydrazine-based systems, through the fact that the fuel and oxidizer show very robust hypergolicity and short ignition delay times, as well as characteristic velocity efficiency (ηC_*) exceeding 98%.

4. Conclusions

With the advent of the "green" or reduced hazards propellants, suitable replacements for the veteran propulsion systems based on hydrazines have been identified. For introduction of new technologies to the very conservative field of space propulsion, the methods presented here offer both continuity in technical concept and reduction in the price.

For the catalytically activated hydrazine monopropellant, a concept has been developed of a dual system for which the decision for actual propellant to be used, whether veteran or comparable "green" propellant, can be delayed. Thus, a smooth technological transfer is enabled, without use of specific high-cost components.

For hypergolically activated bipropellants, a system development has been presented that uses, instead of the risky MMH and N_2O_4, a kerosene-based fuel and hydrogen peroxide oxidizer. Both are nontoxic and in common inexpensive usage in daily life.

DOI: http://dx.doi.org/10.5772/intechopen.82676

Author details

Dov Hasan[1*], Dan Grinstein[1], Alexander Kuznetsov[1], Benveniste Natan[1], Zohar Schlagman[2], Avihay Habibi[2] and Moti Elyashiv[2]

1 Technion – Israel Institute of Technology, Haifa, Israel

2 NewRocket Ltd., Beer Sheva, Israel

*Address all correspondence to: mereagh@technion.ac.il

References

[1] Hasan D, Adler S, Oren A, Miller N. Propulsion systems for small satellites. Space Technology. 1995;**15**(6):375-381

[2] Inbar T. 2008. Available from: http://www.iai.co.il/sip_storage/files/5/36055.wmv to https://he.wikipedia.org/wiki/%D7%A7%D7%95%D7%91%D7%A5:Ofek_7_%2B_launcher.jpg [Accessed: August 29, 2008]

[3] Hasan D, Jaeger M, Oren A, Adler S, Miller N, Zemer E. Application of satellite hydrazine propulsion system in-orbit monitoring model. In: Proc. 4th Int'l Spacecraft Propulsion Conference, ESA SP-555; 2-9 June 2004; Chia Laguna (Cagliari), Sardinia, Italy. 2004

[4] The European Parliament. Registration, Evaluation, Authorisation and Restriction of Chemicals (REACH), Regulation (EC) No 1907/2006; 2006

[5] European Chemicals Agency. Agreement of the Member State Committee on the Identification of Hydrazine as a Substance of Very High Concern; 2011

[6] Gotzig U. Challenges and economic benefits of green propellants for satellite propulsion. In: EUCASS-2017, The 7th European Conference for Aeronautics and Space Sciences; 3-6 July 2017; Milan, Italy. 2017

[7] Anflo K. Concluding a 5 year in-space demonstration of an ADN-based propulsion system on PRISMA. In: Space Propulsion 2016; 2-6 May 2016; Rome, Italy. 2016

[8] Larsson A, Wingborg N. Green propellants based on ammonium dinitramide (ADN). In: Hall J, editor. Advances in Spacecraft Technologies. 2011. Available from: http://cdn.intechweb.org/pdfs/13473.pdf

[9] Wingborg N, de Flon J. Characterization of the ADN-based liquid monopropellant FLP-106. In: Space Propulsion 2010 Conference; 4-8 May 2010; San Sebastian, Spain. 2010

[10] Thormählen P, Anflo K, Sjöberg P, Skifs H. A liquid ADN-based monopropellant for space propulsion. In: Space Propulsion 2010; San Sebastian. 2010

[11] Ek S. Qualification of LMP-103S—An ADN-based satellite propellant. In: Space Propulsion 2016; 2-6 May 2016; Rome, Italy. 2016

[12] Thormählen P. Space qualification of monopropellant LMP-103S. In: Space Propulsion 2016; 2-6 May 2016; Rome. Italy. 2016

[13] Anflo K. High performance green propulsion-on the way for three launches from three continents. In: Space Propulsion 2016; 2-6 May 2016; Rome. Italy. 2016

[14] Persson M. HPGP® a flight proven technology selected for multiple LEO missions. In: Space Propulsion 2016; 2-6 May 2016; Rome, Italy. 2016

[15] Mulkey H, Miller JT, Bacha C. Green propellant loading demonstration at U.S. range, AIAA 2016-4575. In: 52nd AIAA/SAE/ASME Joint Propulsion Conference. Salt Lake City, UT; 2016

[16] Friedhoff P, Hawkins A, Carrico J, Dyer J, Anflo K. On-orbit operation and performance of ammonium dinitramide (ADN) based high performance green propulsion (HPGP) systems, AIAA 2017-4673. In: 53rd AIAA/SAE/ASME Joint Propulsion Conference. Atlanta, GA; 2017

[17] Dinardi A, Anflo K, Friedhoff P, On-Orbit Commissioning of High Performance Green Propulsion (HPGP)

in the SkySat Constellation, Paper SSC17-X-04; Salt Lake City: Small Satellite Conference; 2017

[18] Wurdak M, Strauss F, Werling L, Ciezki H, Greuel D, Lechler R, et al. Determination of fluid properties of the green propellant FLP-106 and related material and component testing with regard to applications in space missions. In: Space Propulsion 2012; Bordeaux. 2012

[19] Negri M, Hendrich C, Wilhelm M, Freudenmann D, Ciezki HK, Gediminas L, et al. Ignition methods for ADN-based liquid monopropellants. In: The EU H2020, New Energetics Workshop; 17-19 May 2016; Sweden: FOI Kista. 2016

[20] Negri M. Replacement of hydrazine: Overview and first results of the H2020 project Rheform. In: 6th European Conference for Aeronautics and Space Sciences (EUCASS). 2015

[21] Negri M, Wilhelm M, Hendrich C, Wingborg N, Gediminas L, Adelöw L, et al. Technology development for ADN-based green monopropellant thrusters—An overview of the RHEFORM project. In: EUCASS-2017, The 7th European Conference for Aeronautics and Space Sciences; 3-6 July 2017; Milan, Italy. 2017

[22] Wilhelm M, Negri M, Hendrich C, Wingborg N, Gediminas L, Adelö L, et al. The RHEFORM project-developments for ADN-based liquid monopropellant thrusters, AIAA 2017-4672. In: 53rd AIAA/SAE/ASME Joint Propulsion Conference. Atlanta, GA; 2017

[23] Hasan D, Grinstein D. Dual capability monopropellant rocket propulsion concept. In: Proceedings of the 58th IACAS-Israel Annual Conference on Aerospace Sciences. 2018. pp. 520-533

[24] Natan B. Advances in gel propulsion, plenary paper ISICP-PL4. In: 11th International Symposium on Special Topics in Chemical Propulsion & Energetic Materials (11-ISICP); September 2018; Stuttgart, Germany. 2018

[25] Lange M, Lein A, Gotzig U, Ziegler T, Anthoine S, Persson M, et al. Introduction of a high-performance ADN based monopropellant thruster on the Myriade propulsion subsystem—Technical and operational concept and impacts, recent advances in space technologies (RAST). In: 6th International Conference on Recent Advances in Space Technologies; 12-14 June 2013; Istanbul, Turkey. 2013

[26] Hasan D, Tavor M, Naveh N, Pavlovsky S, Shechter Y, Oren A, et al. Diaphragm tank based hydrazine systems for long space missions. In: Space Propulsion 2010; 3-6 May 2010; San Sebastian. 2010

[27] Hasan D, Naveh N, Pavlovsky S, Tavor M, Fiksman T, Zaberchik M. Materials compatibility considerations of satellite propellant tanks with EPN-40 diaphragms. In: Space Propulsion 2008, 5-9 May 2008; Heraklion, Crete, Greece. 2008

[28] Bergman G, Anflo K, Dual mode chemical rocket engine and dual mode propulsion system comprising the rocket engine. US Patent Application: 20160115906; 2016

[29] Anflo K, Thormählen P, Persson M. Hot-firing tests using a low temperature derivative of LMP-103S, paper a625. In: EUCASS-2013: 5th European Conf. For Aeronautics and Space Sciences; 1-4 July 2013; Munich, Germany. 2013

[30] Doyle D. Standard Catalog of U.S. Military Vehicles. 2nd ed. Iola, WI: Krause Publications; 2011

[31] Wingborg N, Johansson M, Bodin L. ADN-based liquid monopropellants (presentation). In: ESA 3rd International Conference on Green

Propellants for Space Propulsion; 17-20 September 2006; Poitiers, France. 2006

[32] Beckel S, Dinardi A. High-performance green propulsion (HPGP) for improved performance, responsiveness and reduced lifecycle cost. In: Space Tech Expo, Satellite & Space Summit; 22 May 2013; Long Beach, CA. 2013

[33] Anflo K, Bergman G, Hasanof T, Kuzavas L, Thormählen P, Åstrand B. Flight demonstration of new thruster and green propellant technology on the Prisma satellite, paper SSC07-X-2. In: 21st Annual AIAA/USU Conference on Small Satellites; 13-16 August 2007; Logan: Utah State University. 2007

[34] Hasan D, Yamin S, Reiner D, Gottlieb L, Blummer-Ganon B, Dreerman E, Grinstein D. Report on State of the Art in Alternative (Reduced Hazard) Liquid Propellants for Space Propulsion Rocket Engines, RafDocs#1504523; January 2015; 2015. Unclassified

[35] Amariei D, Courthéoux L, Rossignol S, Batonneau Y, Kappenstein C, Ford M, et al. Influence of fuel on thermal and catalytic decompositions of ionic liquid monopropellants. AIAA Paper 2005-3980. In: 41st AIAA/ASME/ SAE/ASME Joint Propulsion Conference & Exhibit. 2005

[36] Scharlemann C. Green advanced space propulsion—A project status, paper AIAA-2011-5630-890. In: 47th AIAA/ASME/SAE/ASEE Joint Propulsion Conference & Exhibit; San Diego, California. 2011

[37] Robinson JW. Green mono propulsion activities at MSFC, SP2014 paper 2969495. In: Space Propulsion 2014; 18-22 May 2014; Köln, Germany. 2014

[38] Robinson J, Beckel S. Green propulsion auxiliary power unit demonstration at MSFC, SP2014 paper 2925788. In: Space Propulsion 2014; 18-22 May 2014; Köln, Germany. 2014

[39] Thormählen P and Anflo K, Low-temperature operational and storable ammonium dinitramide based liquid. Patent WO2012166046 A2 & A3; 2012

[40] Gotzig U, Telitschkin D, Haecker F, Duelger E. Overview and actual development status of astriums monopropellant thruster family, SP2014 paper 2968006. In: Space Propulsion 2014; 18-22 May 2014; Köln, Germany. 2014

[41] Gotzig U, Ziegler T, Fiot D, Wynn J, Persson M, Anflo K. Astriums alternative propellant activities, SP2014 paper 2968009. In: Space Propulsion 2014; 18-22 May 2014; Köln, Germany. 2014

[42] Welberg D, Lange M, Anflo K, Persson M, Bahu J-M. Conceptual study of a HPGP reaction control system for a launcher upper stage, SP2014 paper 2965218. In: Space Propulsion 2014; 18-22 May 2014; Köln, Germany. 2014

[43] Persson M, Welberg D, Lange M, Bahu J-M, Anflo K. 200N HPGP thruster demonstration for launcher upper stage reaction control system, SP2014 paper 2968097. In: Space Propulsion 2014; 18-22 May 2014; Köln, Germany. 2014

[44] Klapötke TM. Chemistry of High-Energy Materials. Berlin, New York: Walter de Gruyter GmbH; 2011

[45] Hendrich C, Ciezki H, Schlechtriem S, Gernoth A, Wingborg N, Scharlemann C. Influence of water content in an ADN based liquid mono-propellant on performance characteristics. In: Space Propulsion 2014; Köln. 2014

[46] Negri M, Hendrich C, Wilhelm M, Freudenmann D, Ciezki HK, Gediminas L, et al. Thermal ignition of ADN-based propellants, SP2016 paper 3125004. In:

Space Propulsion 2016; 2-6 May 2016; Rome, Italy. 2016

[47] Larsson A, Wingborg N, Elfsberg M, Appelgren P. Characterization and Electrical Ignition of ADN-Based Liquid Monopropellants; FOI-R-1639-SE; 2005

[48] Neff K, King P, Anflo K, Möllerberg R. High performance green propellant for satellite applications. In: 45th AIAA/ASME/SAE/ASEE Joint Propulsion Conference; 2-5 August 2009; Denver, Colorado. 2009

[49] Natan B, Perteghella V, Solomon Y. Hypergolic ignition by fuel gellation and suspension of reactive or catalyst particles. Journal of Propulsion and Power. 2011;**27**:1145

[50] Connell TL Jr, Risha GA, Yetter RA, Natan B. Ignition of hydrogen peroxide with gel hydrocarbon fuels. Journal of Propulsion and Power. 2018;**34**:170

[51] Connell TL Jr, Risha GA, Yetter RA, Natan B. Hypergolic ignition of hydrogen peroxide/gel fuel impinging jets. Journal of Propulsion and Power. 2018;**34**:182

[52] Connell TL Jr, Risha GA, Yetter RA, Natan B. Characterization of gelled hydrocarbon fuels and hydrogen peroxide as a hypergolic bi-propellant. International Journal of Energetic Materials and Chemical Propulsion. 2018;17(1):57-78

[53] Spicer PT, Gilchrist JF. Ch 3b: Microstructure, rheology, and processing of complex fluids. In: Kresta SM, Etchells AW III, Dickey DS, Atiemo-Obeng VA, editors. Advances in Industrial Mixing: A Companion to the Handbook of Industrial Mixing. 1st ed. John Wiley & Sons, Inc.; 2015. Available from: http://www.nonequilibrium.com/pdf/NAMFMixingRheologyChapter.pdf

[54] Beris A, Tsamopoulos J, Armstrong R, Brown R. Creeping motion of a sphere through a Bingham plastic. Journal of Fluid Mechanics. 1985;**158**:219-244. Available from: https://www.cambridge.org/core/services/aop-cambridge-core/content/view/58DA7E990C0D389D714EC311337CB0E0/S0022112085002622a.pdf/creeping_motion_of_a_sphere_through_a_bingham_plastic.pdf

[55] Chhabra RP. Bubbles, Drops, and Particles in Non-Newtonian Fluids. Boca Raton, FL: CRC Press, Taylor & Francis; 2007. Available from: https://www.taylorfrancis.com/books/9781420015386

[56] TA Instruments. Rheometers Brochure (RH075B). Available from: http://www.tainstruments.com/pdf/literature/ar2000.pdf [Accessed: July 12, 2017]

[57] Ciezki HK, Kirchberger C, Stiefel A, Kröger P, Caldas Pinto P, Ramsel J, et al. Overview on the German gel propulsion technology activities: Status 2017 and outlook. In: EUCASS-2017, the 7th European Conference for Aeronautics and Space Sciences; 3-6 July 2017; Milan, Italy. 2017